Effects of Increasing Acidity on Metal(loid) Bioprecipitation in Groundwater: Column Studies

ARTICLE *in* ENVIRONMENTAL SCIENCE AND TECHNOLOGY · NOVEMBER 2007

Impact Factor: 5.33 · DOI: 10.1021/es071122v · Source: PubMed

Environ. Sci. Technol. **2007**, *41,* 7131−7137

Effects of Increasing Acidity on Metal(loid) Bioprecipitation in Groundwater: Column Studies

ALEXANDER C. DAVIS,[†,‡]
BRADLEY M. PATTERSON,[*,‡]
MICHELLE E. GRASSI,[§]
BLAIR S. ROBERTSON,[‡]
HENNING PROMMER,[‡] AND
ALLAN J. MCKINLEY[||]

Department of Chemistry, Purdue University, West Lafayette, Indiana 47907-2084, CSIRO Land and Water, Private Bag No. 5, Wembley, WA 6913, Australia, Environmental Resources Management (Australia), P.O. Box 266, South Melbourne, VIC, 3205, Australia, and Faculty of Life and Physical Sciences, University of Western Australia, Crawley, WA 6907, Australia

Large-scale column experiments were carried out over a period of 545 days to assess the effect of increasing acidity on bacterial denitrification, sulfate reduction, and metal(loid) bioprecipitation in groundwater affected by acid mine drainage. At a groundwater pH of 5.5, denitrification and Cu^{2+} removal, probably via malachite ($Cu_2(OH)_2CO_3$) precipitation, were observed in the ethanol-amended column. Sulfate reduction, sulfide production, and Zn^{2+} removal were also observed, with Zn^{2+} removal observed in the zone of sulfate reduction, indicating likely precipitation as sphalerite (ZnS). Se^{6+} removal was also observed in the sulfate reducing zone, probably as direct bioreduction to elemental selenium via ethanol/acetate oxidation or sulfide oxidation precipitating elemental sulfur. A step decrease in groundwater pH from 5.5 to 4.25 resulted in increased denitrification and sulfate reduction half-lives, migration of both these redox zones along the ethanol-amended column, and the formation of an elevated Cu^{2+} plume. Additionally, an elevated Zn^{2+} plume formed in the previous sulfate reducing zone of the ethanol-amended column, suggesting dissolution of precipitated sphalerite as a result of the reduction in groundwater pH. As Cu^{2+} passed through the zone of sphalerite dissolution, SEM imaging and EDS detection suggested that Cu^{2+} removal had occurred via chalcocite (Cu_2S) or covellite (CuS) precipitation.

Introduction

Traditional remediation treatment methods for groundwater contaminated with acid mine drainage (AMD), such as pump and treat methods, can be costly and may need to be maintained for many years, depending on the extent of the contamination (*1*). Recently, bioprecipitation using sulfate-reducing bacteria (SRB) as a possible remediation method has received a great deal of attention (*2*−*6*). Under favorable biogeochemical conditions SRB will catalyze the oxidation of organic compounds such as ethanol (partially or completely) with the reduction of sulfate to sulfide (eq 1).

$$2CH_3CH_2OH + 3SO_4^{2-} + 3H^+ \rightarrow 3HCO_3^- + 3H_2S + 3H_2O + CO_2 \quad (1)$$

Metal ions that might be present in groundwater can then form stable, insoluble metal sulfides in the presence of hydrogen sulfide (eq 2).

$$H_2S + Metal^{2+} \rightarrow MetalS_{(s)} + 2H^+ \quad (2)$$

Bioprecipitation treatment engineered as a permeable reactive barrier (PRB) has the potential to be an effective method for treatment of AMD (*3*, *6*). Investigation of the effect of pH on metal mobility has shown reduced metal sorption to bacterial biomass (*7*) and sediment (*8*) under acidic conditions. Also, pH conditions can affect the efficiency of sulfate-reducing bacteria, with longer periods of acclimation and reduced sulfate reduction rates under increasing acidic conditions (*5*, *9*). However, a detailed assessment of the effects of changing pH conditions (that may be associated with variable field conditions) to an active bioprecipitation process has not been undertaken. This paper reports on the results of a 545 day large-scale column experiment investigating the effect of a step decrease in groundwater pH on the bioprecipitation of metal(loid) contaminants, to assess the robustness of the bioprecipitation process.

Materials and Methods

Column Experiment. Two polyvinyl chloride (PVC) columns were constructed (1.9 m long, 15 cm i.d.) with 13 sampling ports fitted along the columns at regular intervals (see Figure S1 in the Supporting Information). A polymer mat, used for ethanol amendment, was installed 0.51 m from the base of each column. The columns were filled with a highly bleached, low organic (200 mg kg^{-1}) and iron (13 mg kg^{-1}) content sand collected from the Swan Coastal Plain, Perth, Western Australia. Local Perth groundwater containing sulfate (∼ 30−50 mg L^{-1} SO_4^{2-} as S), nitrate (∼ 4−10 mg L^{-1} NO_3^- as N), and dissolved oxygen (∼ 2.1 mg L^{-1}) with a low dissolved organic carbon (DOC) content (∼ 4 mg L^{-1} as C) was used. Detailed groundwater chemistry is given in Prommer et al. (*10*). The groundwater was spiked with a concentrated metal(loid) chloride and sodium/hydrogen selenate solution to give a final concentration of 12 mg L^{-1} for Zn^{2+}, 4.0 mg L^{-1} for Cu^{2+}, and 1.2 mg L^{-1} for Se^{6+}. The pH was initially maintained at 5.5 via HCl/NaOH addition. An upward groundwater flow was delivered by a hydraulic head on the columns between 1 and 1.5 m over the duration of the experiment. The volumetric flow through each column was regulated by a peristaltic pump on the effluent line to give a flow rate of approximately 0.25 mL min^{-1} (effective groundwater velocity of ∼29 m y^{-1}, typical of local groundwater velocity). The experiment was conducted at room temperature, which was coarsely controlled to 22 °C.

Prior to ethanol amendment, metal(oid)-spiked groundwater and bromide (200 mg L^{-1} as Br) was passed through the columns to determine metal(oid) retardation and soil porosity. Once the metal(loid) aqueous concentrations were evenly distributed throughout the lengths of both columns, ethanol was continuously added to one column while the other column was maintained without carbon addition as a control. The control column was used to differentiate sorption-only processes from precipitation processes. Also, column experiments were run for extended periods to enable

* Corresponding author e-mail: bradley.patterson@csiro.au; phone: +61 8 9333 6276; fax: +61 8 9333 6211.
† Purdue University.
‡ CSIRO Land and Water.
§ Environmental Resources Management (Australia).
|| University of Western Australia.

10.1021/es071122v CCC: $37.00
Published on Web 09/11/2007

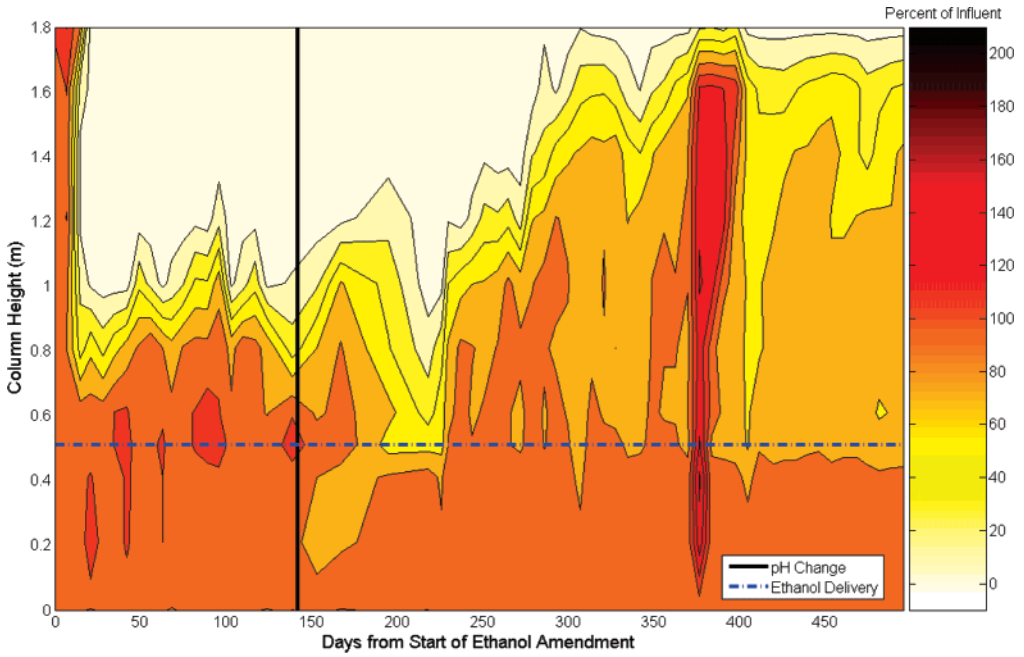

FIGURE 1. Nitrate concentration as percent of influent in the ethanol-amended column.

column processes to reach pseudo-equilibrium to also better differentiate sorption and precipitation processes. Once bioprecipitation was established, the effect on the bioprecipitation process of a step reduction in influent groundwater pH from 5.5 to 4.25 was assessed.

Ethanol Amendment. Ethanol was delivered to the ethanol-amended column via diffusion from a polymer mat (*6*, *11*, *12*) located 0.51 m from the base of the column, emplaced perpendicular to the direction of flow within the circumference of the column. The polymer mat was constructed of 5 m of poly(dimethylsiloxane) tubing (3.0 mm o.d., 2.0 mm i.d.), which contained coiled stainless steel wire inside the tubing to prevent collapse. The tubing was woven into a 13.5 cm diameter flexible plastic support frame to prevent twisting of the mat. For ethanol amendment, a concentrated ethanol solution (5−15 g L^{-1}) was pumped through the lumen of the polymer tube at a rate of 2 mL min^{-1} to give an ethanol groundwater concentration of 0.8−1.6 g L^{-1} at the point of amendment.

Groundwater Analysis and Soil Mineralogy. Groundwater samples (35 mL) were collected weekly from both columns using 65 mL plastic syringes. Groundwater subsamples were acidified and analyzed for ethanol and degradation products (acetate, propionate, butyrate) by direct aqueous injection gas chromatography using a BP 21 capillary column (25 m, 0.32 mm internal diameter, 0.25 μm film thickness) with flame ionization detection (FID) (*14*). Groundwater subsamples for sulfide (S^{2-} and H_2S) were determined colorimetrically after the formation of a colloidal copper sulfide precipitate (*15*). Analysis for nitrate and sulfate was conducted using high-performance liquid chromatography (HPLC); Cu^{2+} and Zn^{2+} analyses were conducted using a Varian AA-40 atomic absorption spectrophotometer (AAS); pH, dissolved oxygen, and reduction potential (Eh) were measured using specific electrodes. Se^{6+} analysis was conducted using an Agilent 7500cs inductively coupled plasma mass spectrometer (ICP−MS) once stable sulfate-reducing conditions were achieved, and at the end of the experiment after a step pH reduction. Details of the analytical methods are given in Davis (*16*).

The soil used in the column experiment (blank soil sample) was analyzed by X-ray diffraction (XRD) to determine the major mineralogical composition. XRD patterns were recorded with a Philips PW1800 microprocessor-controlled diffractometer using Co Kα radiation, variable divergence slit, and graphite monochromator. The diffraction patterns were recorded in steps of 0.05° 2θ with a 1.0 s counting time per step and logged to data files for analysis. Quantitative analysis was performed on the XRD data using the commercial package SIROQUANT from Sietronics Pty Ltd.

At the completion of the column experiment, soil samples were collected and analyzed by X-ray fluorescence (XRF) and scanning electron microscopy (SEM) with an energy dispersive spectroscopy (EDS) detector.

The major and trace element geochemistry of the soil samples was determined using XRF on fused glass disks. Soil samples for XRF were mixed in a 12−22 ratio with lithium borate flux and the mixture was heated to 1050 °C in a Pt/Au crucible for 12 min. The resulting glass disks were analyzed on a Philips PW1480 wavelength dispersive XRF system using a dual anode Sc/Mo tube. SEM imaging was conducted using a Zeiss 1555 SUPRA variable pressure instrument equipped with an Oxford Instruments energy dispersive spectroscopy (EDS) detector. The accelerating voltage used was 15 keV, with an object aperture of approximately 30 μm at working distances between 12 and 17 mm. A system vacuum of 1.89 × 10^{-5} Torr was maintained during analysis.

Results and Discussion

Establishment of Denitrification and Sulfate-Reducing Conditions. Fourteen days after ethanol amendment commenced, significant denitrification (60% reduction in NO_3^- concentration) was observed between 0.81 and 1.61 m from the base of the column. Within 1 month of ethanol amendment, denitrification had stabilized in a zone between 0.81 and 1.01 m from the base of the column with denitrification half-lives ranging between 0.73 and 2.9 days (Figure 1). In this denitrifying zone, 98−99% of Cu^{2+} was removed from the groundwater (Figure 2).

Under near steady-state conditions, a zone of elevated pH (1.3 pH units greater than the influent) was observed in the zone of denitrification/Cu^{2+} removal (Figure 3). The inception of this elevated pH zone coincided with the start of denitrification. The Cu^{2+} removal observed in the denitrification zone before sulfate reduction commenced could have been due to the following: (i) an increase in Cu^{2+} sorption onto the soil as a result of the elevation in pH; (ii)

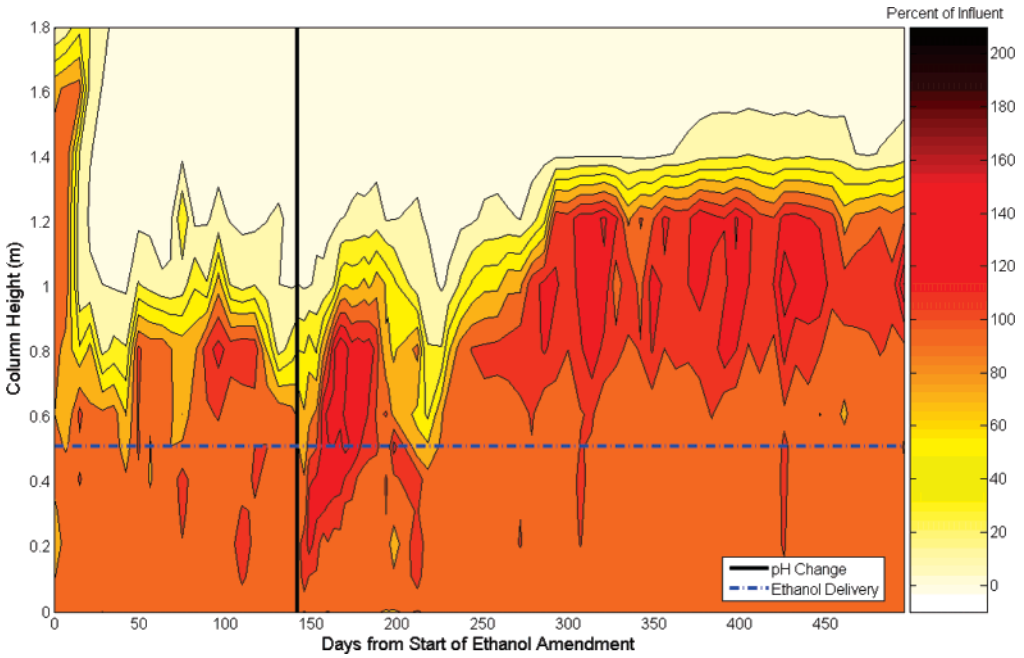

FIGURE 2. Cu^{2+} concentration as percent of influent in the ethanol-amended column.

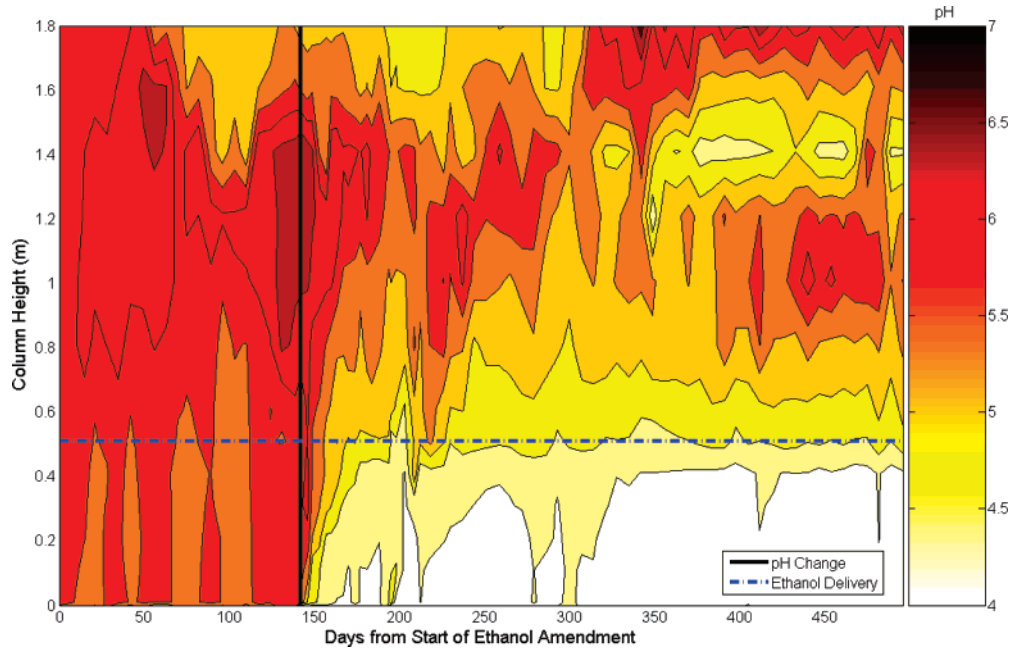

FIGURE 3. pH values in the ethanol-amended column.

biosorption of Cu^{2+} to denitrifying bacteria (*7*); (iii) formation of malachite ($Cu_2(OH)_2CO_3$) in a carbonate rich zone (*13*) as a result of carbonate production from ethanol oxidation/denitrification; or (iv) through the abiotic reduction of Cu^{2+} to elemental Cu as a result of the decrease in groundwater reduction potential. The removal of Cu^{2+} via sorption would be a transient process and would be expected to cease once sorption capacity was reached, therefore the formation of malachite or elemental Cu would be more likely. A detailed biogeochemical transport modeling study (*10*) has been undertaken to further elucidate the abiotic and biotic processes occurring within the column. This modeling indicated the formation of malachite within the denitrification zone was possible, while the reduction to elemental Cu would occur, but downgradient of the denitrification zone.

As the ethanol-amended column was not destructively soil sampled during this stage of the experiment, definitive soil chemistry data for malachite formation was not available. However, the combined data of (i) observed bicarbonate (from 6 to 73 mg L^{-1}) production corresponding to the location of Cu^{2+} removal (see Figure S2 in the Supporting Information); (ii) geochemical modeling showing malachite to be the only mineral oversaturated under these aqueous chemical conditions (*10*); and (ii) the previously observed malachite precipitation under similar geochemical conditions (*13*), suggests that malachite precipitation was the likely mechanism for Cu^{2+} removal.

Sulfate reduction indicated by a decrease in sulfate concentration (Figure 4) and production of sulfide (Figure S3 in the Supporting Information), was first observed 1.81 m from the base of the column, 56 days after ethanol amendment commenced. The first substantial removal of Zn^{2+} (98% removal) corresponded in both time and column location to the onset of sulfate reduction (Figure 5). Between

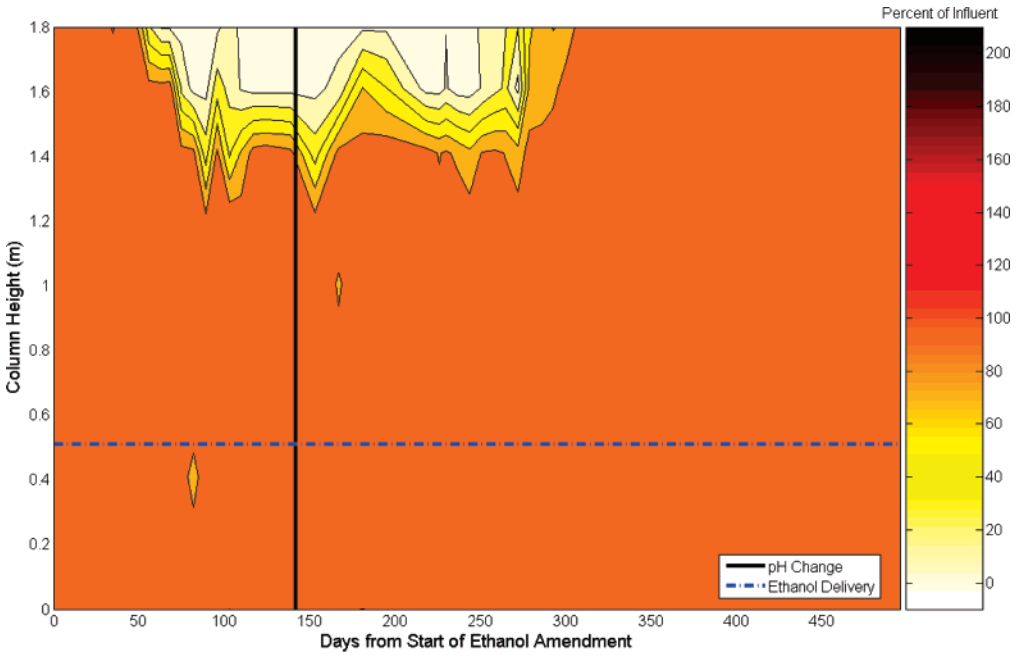

FIGURE 4. Sulfate concentration as percent of influent in the ethanol-amended column.

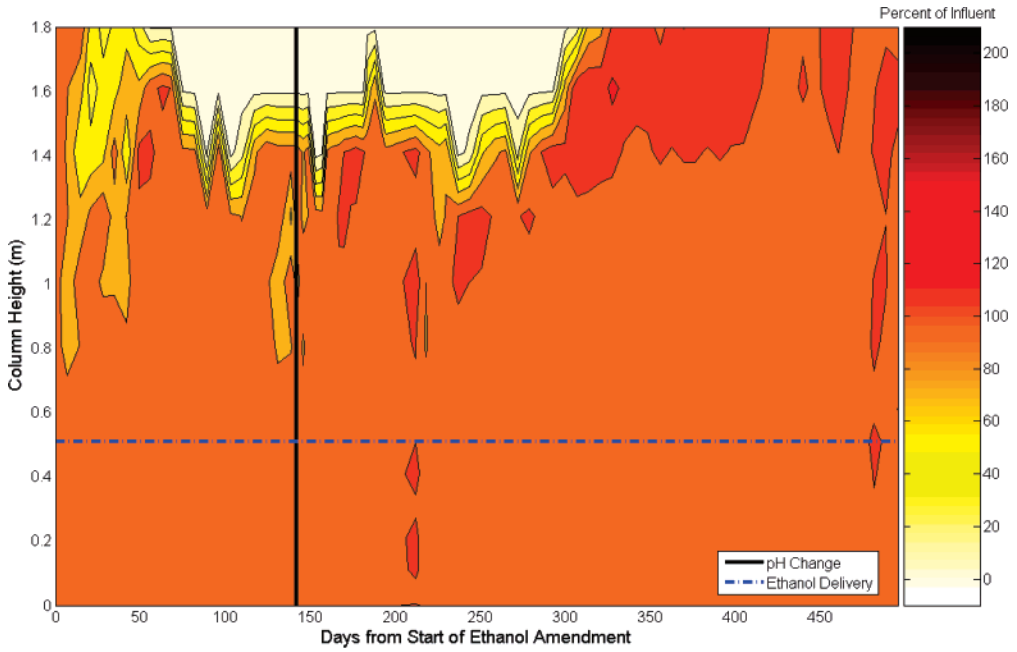

FIGURE 5. Zn^{2+} concentration as percent of influent in the ethanol-amended column.

days 63 and 140, stable sulfate reduction (with sulfate concentrations reduced from ~40 mg L^{-1} to <2 mg L^{-1}) and Zn^{2+} removal zones were observed between 1.41 and 1.61 m. During this time, sulfide (S^{2-} and H_2S) production accounted for ~70% of the sulfate removal. The Zn^{2+} removal observed in the sulfate-reducing zone was most likely due to the formation of zinc sulfide. Se^{6+} removal was also observed in the sulfate-reducing zone (see Figure S6 in the Supporting Information). The possible mechanism for Se^{6+} removal was either (i) microbiological reduction of Se^{6+} to elemental selenium via ethanol/acetate oxidation (*17*) or sulfide oxidation to elemental sulfur (*18*), or (ii) formation of nonvolatile organic selenides (*19*).

There was also a zone of decreased pH (1.2 pH units) in the zone of sulfate reduction between 1.61 and 1.81 m starting about day 63 (Figure 3). In this zone, the incomplete oxidation of ethanol to acetic acid (eq 3) was observed (Figures S4 and S5 in the Supporting Information), possibly accounting for the decrease in pH.

$$2\ CH_3CH_2OH + SO_4^{2-} \rightarrow 2\ CH_3COOH + S^{2-} + 2\ H_2O \qquad (3)$$

The redox potential of effluent groundwater from the ethanol-amended column reflected the changes in geochemistry within the column. Redox potential (Eh), initially at approximately 240 mV, decreased to approximately 100 mV once denitrification commenced, then to −160 mV with the onset of sulfate reduction, and stabilized at approximately −210 mV, 28 days later (see Figure S7 in the Supporting Information).

Step pH Reduction. One hundred forty-two days after the commencement of ethanol amendment, when a steady-state redox-zonation and metal bioprecipitation had been established for over 67 days, the pH of the metal(loid)-

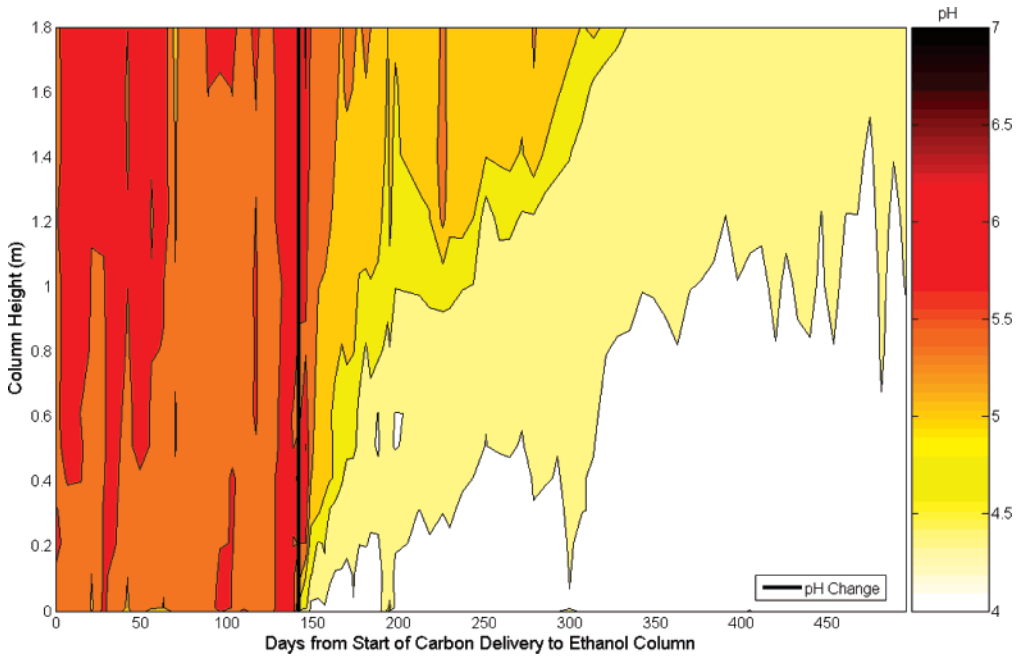

FIGURE 6. pH values in the control column.

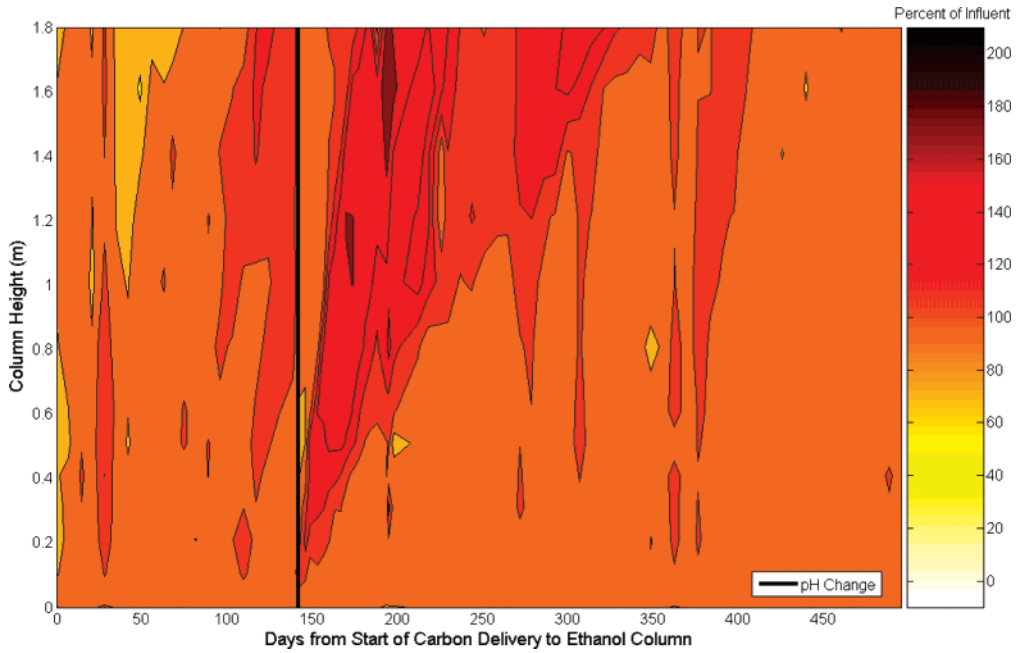

FIGURE 7. Cu^{2+} concentration as percent of influent in the control column.

contaminated influent groundwater was decreased from 5.5 to 4.25 via the addition of HCl. The reduced pH front was observed to migrate along the control column for approximately 210 days (Figure 6), at which time the pH was approximately uniform along the entire column. The low pH migration velocity (3.6 m y^{-1}) was about eight times lower than the column groundwater velocity (29 m y^{-1}), and was likely the result of the relatively small decrease in groundwater pH combined with the buffering by calcite in the soil (soil calcite concentration was 2.9 mg kg^{-1}, based on quantitative XRD analysis). This slow pH front migration was also observed in the ethanol-amended column (Figure 3). However, the pH front migration in the ethanol-amended column was confounded by the biological and geochemical changes associated with denitrification, sulfate reduction, and ethanol oxidation.

In both the control and ethanol-amended columns, the formation of a plume of elevated Cu^{2+} concentration (Figures 7 and 2) was observed, in conjunction with the migration of the pH front. The plumes of elevated Cu^{2+} concentration migrated along the columns at a velocity similar to that of the pH front. The formation of these increased plumes was most likely the result of Cu^{2+} desorption from the soil as a result of the decrease in groundwater pH. Batch sorption tests (*16*) gave K_d values for Cu^{2+} of 1.1 L kg^{-1} at pH 5.4 and 0.16 L kg^{-1} at pH 4.2 (see Figure S8 in the Supporting Information). Additionally, dissolution of malachite or desorption from denitrifying bacteria may also have occurred in the ethanol-amended column. Esposito et al. (*7*) observed a decrease in Cu^{2+} sorption to certain biomass with a decrease in pH. Dissolution of copper sulfide minerals was an unlikely mechanism for the elevated Cu^{2+} concentration, as these

minerals were unlikely to form since the Cu^{2+} removal occurred upgradient of the sulfate-reducing zone.

In the control column, by day 364 (224 days after the step reduction in pH), the Cu^{2+} concentration along the length of the control column had reduced to concentrations similar to that of the influent (Figure 7). There were no observable changes in nitrate, sulfate, or Zn^{2+} concentrations in the control column over the experimental period. In the ethanol-amended column, as the pH front migrated along the column, the denitrification, Cu^{2+} removal, sulfate reduction, and Zn^{2+} removal zones were also observed to migrate along the column. As the pH front migrated into the denitrifying zone, the denitrifying zone was observed to migrate from 0.81 to 1.61 m between day 230 and 349, with an increase in denitrification half-lives from 0.8−2.6 days (at steady state) to 2.8−7.8 days. Along with the migration of the denitrification zone, the Cu^{2+} removal zone migrated from 0.81 to 1.41 m.

As the pH front migrated into the sulfate-reducing zone, sulfate reduction half-lives increased from between 0.3 and 1 day to 8 days. Both Zn^{2+} removal and sulfate-reduction zones also migrated along the column from 1.41 m to beyond the final sampling port (1.81 m) of the column. Three hundred fifteen days after ethanol amendment commenced, no sulfate reduction or Zn^{2+} bioprecipitation was observed in the ethanol-amended column. Also, an elevated Zn^{2+} concentration plume (>110% of influent concentration) emanating from the previous sulfate-reducing zone (1.41 m) was observed. It was unlikely that desorption of Zn^{2+} from the soil could have caused the increased Zn^{2+} concentrations, as batch sorption tests showed no observable difference in Zn^{2+} K_d values between pH 4.2 and 6.0 (see Figure S8 in the Supporting Information). Also, no increase in Zn^{2+} concentration was observed in the control column after the decrease in pH. Therefore, the enhanced Zn^{2+} concentration plume was likely due to dissolution of precipitated sphalerite (ZnS) as a result of the reduced pH conditions, while the inhibition of sulfate-reducing bacteria (*5*, *9*) and the corresponding lack of sulfide production at that location prevented further Zn^{2+} bioprecipitation. Nelson et al. (*20*) observed a similar remobilization of molybdenum anaerobic biotreatment byproducts under less reductive conditions.

By day 300 (160 days after the step reduction in pH), the Cu^{2+} removal zone had restabilized at 1.41 m (within the previously observed sulfate-reducing zone), while the denitrification zone continued to migrate downgradient. By day 350, denitrification had restabilized at 1.61 m. The discrete Cu^{2+} removal zone (1.41 m) and denitrification zone (1.61 m) between day 350 and 504 indicated that the mechanism for Cu^{2+} removal during this time was not the formation of malachite ($Cu_2(OH)_2CO_3$) as a result of carbonate production from ethanol oxidation/denitrification. As the Cu^{2+} removal zone migrated into the previous sulfate-reduction zone, an increase in the groundwater Zn^{2+} concentration was observed at this location. Based on the prolonged (>200 days) Cu^{2+} removal and increased Zn^{2+} concentration (maximum of 135% of the influent concentration) together with no observed sulfide (<2 mg L^{-1}) production during this period, it was postulated that the reduction in groundwater pH resulted in the dissolution of sphalerite (ZnS) and that the released sulfide reacted with the dissolved Cu^{2+} to precipitate the less acid soluble copper sulfide minerals, chalcocite (Cu_2S) or covellite (CuS).

Soil Geochemistry. At the completion of the column experiments (504 days after ethanol amendment commenced), the columns were destructively sampled and soil samples were collected from the ethanol-amended column at 1.4 m (the observed location of sulfate reduction during steady state at pH 5.5, and later the observed location of Cu^{2+} removal during steady state at pH 4.25) and from 1.9 m (near the column effluent). Additionally, a soil sample

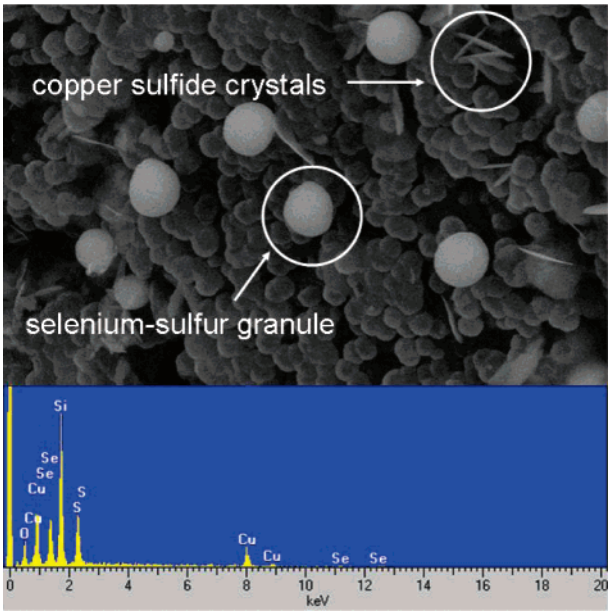

FIGURE 8. SEM image (28 000× mag) of soil collected from 1.4 m in the ethanol-amended column, and corresponding EDS.

was collected from the control column at 1.4 m (control soil sample), and a soil sample collected prior to packing the columns (blank soil sample).

XRF analyses indicated that both the blank and the control soil samples did not contain substantial quantities of either copper or zinc (see Table S1 in the Supporting Information). Selenium was unable to be quantified due to tungsten contamination from the grinding mill during XRF sample preparation. However, in the soil samples collected from the ethanol-amended column after the completion of the column experiment, elevated soil zinc concentrations were observed at 1.4 m (33 mg kg^{-1}) and 1.9 m (142 mg kg^{-1}), consistent with sulfate reduction migrating from 1.4 m to beyond the last sampling port as the pH front progressed along the ethanol-amended column. The elevated soil zinc concentrations, together with the prolonged increased effluent Zn^{2+} concentration, indicated that complete ZnS dissolution had not occurred by the end of the column experiment. Elevated soil copper concentrations were observed at 1.4 m (189 mg kg^{-1}), but not at 1.9 m (<14 mg kg^{-1}), which was consistent with groundwater chemical data that indicated Cu^{2+} removal was occurring between 1.2 and 1.4 m for days 293−504 of ethanol amendment (Figure 2).

Soil SEM Analysis. SEM images and corresponding EDS for soil samples were collected from the control column at 1.4 m and from the ethanol-amended column at 1.4 and 1.9 m. The SEM image and EDS for the control column soil sample (see Figure S9 in the Supporting Information) indicated no observable formation of minerals on the sand particles.

The SEM image for the soil sample collected from the ethanol-amended column at 1.4 m showed both spherical micrometer-sized granules along with micrometer-sized crystalline needles (Figure 8). The EDS identified copper, sulfur, and selenium as major elements of the minerals deposited on the sand particles. However, no zinc minerals were detected by EDS, which may have been due to sphalerite (ZnS) dissolution under low pH conditions from this location (Figure 8). The spherical micrometer-sized granules were consistent with selenium spheres observed by Oremland et al. (*21*) and selenium−sulfur granules observed by Hockin and Gradd (*18*) under reducing conditions. These data are consistent with the groundwater chemical data that showed Se^{6+} removal in the sulfate-reducing zone (see Figure S6 in

the Supporting Information). The micrometer-sized crystalline needles were consistent with copper sulfide, possibly chalcocite (Cu_2S) or covellite (CuS) which form parallel rows of crystals and are often intermixed (*22*). The formation of copper sulfide minerals at 1.4 m may be the result of the dissolution of sphalerite (ZnS) that had previously formed (between days 56 and 250) under sulfate-reducing conditions, coupled with the presence of Cu^{2+} between day 350 and 504.

The SEM image for the soil sample collected from the ethanol-amended column at 1.9 m (see Figure S10 in the Supporting Information) showed spherical micrometer-sized granules. Unfortunately, due to the charging of the soil particles by the SEM's electron beam, a clearer image of the soil sample from 1.90 m was not obtained. The EDS identified zinc, sulfur, and selenium as major elements of the minerals deposited on the sand particles. The spherical micrometer-sized granules were consistent with both selenium−sulfur granules (*18*) and sphalerite (*23*).

Implications for Field Application. Under steady-state mildly acidic conditions, bioprecipitation of metal(loid)-contaminated groundwater via ethanol oxidation and denitrification/sulfate reduction was shown to be a feasible remediation strategy for Cu^{2+}, Zn^{2+}, and Se^{6+}. However, this *in situ* biological remediation process may be too sensitive to cope with variable field conditions, especially where occasional additional acidic fluxes occur. Under these conditions, there is potential for dissolution of previously precipitated minerals and further migration of a metal(loid) contamination plume.

Acknowledgments

We thank Luke Zappia for assistance conducting the SEM. Thanks also to J. Plumb and G. Douglas for critically reviewing early drafts of this manuscript. This work was partially funded by Rio Tinto.

Supporting Information Available

Additional figures and a table. This material is available free of charge via the Internet at http://pubs.acs.org.

Literature Cited

(1) Elliott, P.; Ragusa, S.; Catcheside, D. Growth of sulfate-reducing bacteria under acidic conditions in an upflow anaerobic bioreactor as a treatment system for acid mine drainage. *Water Res.* **1998**, *32* (12), 3724−3730.

(2) Harris, M. A.; Ragusa, S. Bacterial mitigation of pollutants in acid drainage using decomposable plant material and sludge. *Environ. Geol.* **2000**, *40* (1−2), 195−215.

(3) Waybrant, K. R.; Blowes, D. W.; Ptacek, C. J. Selection of reactive mixtures for use in a permeable reactive wall for the treatment of mine drainage. *Environ. Sci. Technol.* **1998**, *32* (13), 1972−1979.

(4) Utgikar, V. P.; Tabak, H. H.; Haines, J. R.; Govind, R. Quantification of toxic and inhibitory impact of copper and zinc on mixed cultures of sulfate-reducing bacteria. *Biotechnol. Bioeng.* **2003**, *82* (3), 306−312.

(5) Tsukamoto, T. K.; Killion, H. A.; Miller, G. C. Column experiments for microbial treatment of acid mine drainage: low-temperature, low-pH and matrix investigations. *Water Res.* **2004**, *38*, 1405−1418.

(6) Patterson, B. M.; Yamin M., Grassi, M. E.; Robertson, B. S.; Davis, G. B.; Lipman, M.; Rhodes, S.; Mckinley, A. J.; Rate, A. W. Assessment of different carbon sources and delivery techniques to promote an *in situ* reactive zone for bioprecipitation of metals in groundwater. In *Permeable Reactive Barriers*; Boshoff, G. A., Bone, B. D., Eds.; IAHS Press: Oxfordshire, U.K., 2005; pp 97−104.

(7) Esposito, A.; Pagnanelli, F.; Lodi, A.; Solisio, C.; Vegliò, F. Biosorption of heavy metals by *Sphaerotilus natans*: an equilibrium study at different pH and biomass concentrations. *Hydrometallurgy* **2001**, *60*, 129−141.

(8) Elzahabi, M.; and Yong, R. N. pH influence on sorption characteristics of heavy metals in the vadose zone. *Eng. Geol.* **2001**, *60*, 61−68.

(9) Tucker, M. D.; Barton, L. L.; Thomson, B. M. Reduction of Cr, Mo, Se and U by *Desulfovibrio desulfuricans* immobilized in polyacrylamide gels. *J. Ind. Microbiol. Biotechnol.* **1998**, *20* (1), 13−19.

(10) Prommer, H.; Grassi, M. E.; Davis, A. C.; Patterson, B. M. Modeling of microbial dynamics and geochemical changes in a metal bioprecipitation experiment. *Environ. Sci. Technol.* (Submitted).

(11) Patterson, B. M.; Grassi, M. E.; Davis, G. B.; Robertson, B.; McKinley, A. J. The use of polymer mats in series for sequential reactive barrier remediation of ammonium-contaminated groundwater: Laboratory column evaluation. *Environ. Sci. Technol.* **2002**, *36*, 3439−3445.

(12) Grassi, M. E.; Patterson, B. M.; Davis, G. B.; Robertson, B. S.; McKinley, A. J. Estimation of ethanol mass delivery to groundwater from silicone polymer mats. *Environ. Sci. Technol.* **2007**, *41* (15), 5453−5459.

(13) Ludwig, R. D.; McGregor, R. G.; Blowes, D. W.; Benner, S. G.; Mountjoy, K. A permeable reactive barrier for treatment of heavy metals. *Ground Water* **2002**, *40* (1), 59−66.

(14) Carlsson, J. Simplified Gas Chromatographic Procedure for Identification of Bacterial Metabolic Products. *Appl. Environ. Microbiol.* **1973**, *25* (2), 287−289.

(15) Cord-Ruwisch, R. A quick method for the determination of dissolved and precipitated sulphides in cultures of sulphate-reducing bacteria. *J. Microbiol. Methods* **1985**, *4*, 33−36.

(16) Davis, A. C. Effects of acidity on bacterial sulfate reduction and metal bioprecipitation in acid rock drainage groundwater using three different carbon sources. Masters Thesis, Faculty of Life and Physical Sciences, University of Western Australia, 2005.

(17) Oremland, R. S.; Herbel, M. J.; Switzer Blum, J.; Langley, S.; Beveridge, T. J.; Ajayan, P. M.; Sutto, T.; Ellis, A. V.; Curran, S. Structural and spectral features of selenium nanospheres produced by Se-respiring bacteria. *Appl. Environ. Microbiol.* **2004**, *70* (1), 52−60.

(18) Hockin, S. L.; Gadd, G. M. Linked redox precipitation of sulfur and selenium under anaerobic conditions by sulfate-reducing bacterial biofilms. *Appl. Environ. Microbiol.* **2003**, *69* (12), 7063−7072.

(19) Losi, M. E.; Frankenberger, W. T., Jr. Bioremediation of selenium in soil and water. *Soil Sci.* **1997**, *162* (10), 692−702.

(20) Nelson, B. N.; Cellan, R.; Mudder, T.; Whitlock, J.; Waterland, R. In situ, Anaerobic, Biological Immobilization of Uranium, Molybdenum and Selenium in an Alluvial Aquifer. *Min. Eng.* **2003**, *55* (3), 31−36.

(21) Oremland, R. S.; Hollibaugh, J. T.; Maest, A. S.; Presser, T. S.; Miller, L. G.; Culbertson, C. W. Selenate reduction to elemental selenium by anaerobic bacteria in sediments and culture: Biogeochemical significance of a novel, sulfate-independent respiration. *Appl. Environ. Microbiol.* **1989**, *55* (9), 2333−2343.

(22) Nesse, W. D. Sulfides and Related Minerals. In *Introduction to Mineralogy*; Oxford University Press: Oxford, 2000.

(23) Labrenz, M.; Druschel, G. K.; Thomsen-Ebert, T.; Gilbert, B.; Welch, S. K.; Kemner, K.; Logan, G. A.; Summons, R.; De Stasio, G.; Bond, P. L.; Lai, B.; Kelley, S. D.; Banfield, J. F. Formation of sphalerite (ZnS) deposits in natural biofilms of sulfate-reducing bacteria. *Science* **2000**, *290*, 1744−1747.

Received for review May 14, 2007. Revised manuscript received July 24, 2007. Accepted July 25, 2007.

ES071122V